International Journal of Mechanical, Industrial and Aerospace Sciences
ISSN: 2517-9950
Vol:9, No:4, 2015

# Optimum Turbomachine Selection for Power Regeneration in Vapor Compression Cool Production Plants

S. B. Alavi, G. Cerri, L. Chennaoui, A. Giovannelli, S. Mazzoni

***Abstract*—**Power Regeneration in Refrigeration Plant concept has been analyzed and has been shown to be capable of saving about 25% power in Cryogenic Plants with the Power Regeneration System (PRS) running under nominal conditions. The innovative component Compressor Expander Group (CEG) based on turbomachinery has been designed and built modifying CETT compressor and expander, both selected for optimum plant performance. Experiments have shown the good response of the turbomachines to run with R404a as working fluid. Power saving up to 12% under PRS derated conditions (50% loading) has been demonstrated. Such experiments allowed predicting a power saving up to 25% under CEG full load.

***Keywords*—**Compressor, Expander, Power Saving, Refrigeration Plant, Turbine, Turbomachinery Selection, Vapor Pressure Booster.

## I. Introduction

VAPOR compression based refrigeration plants are worldwide extensively used for domestic applications, air conditioning and industrial processes. The various applications are characterized by different values of the evaporator temperature and working fluids. While the upper condensing temperatures depend on the environment, into which the Heat Power (HP) is rejected. An enormous amount of electric energy (also primary energy) is worldwide consumed by the various plants whose Cool Power (CP) ranges from a few hundred Watts to more than 10 MW per unit. The worldwide consumed electric energy by Vapor Compression Refrigeration Systems (VCRSs) is an enormous quantity being some 15%, corresponding to some 4.5% of the greenhouse effect total gas emissions. The millions liters (huge value) of fossil fuels (gasoline, diesel fuel, liquigas, natural gas and coal) that are burned to power air conditioners and refrigerators for cars, trucks and ships, must be added to the above consumption [1], [2]. It can be easily understood that a small percentage of power saving per unit of produced cool leads to saving an enormous amount of primary energy and of $CO_2$ and other pollutant emissions. For these reasons, there is continuous search to improve the VCRS Coefficient of Performance (COP) through the definition of new refrigerants and the implementation of innovations in the cycle arrangements introducing new devices. Fig. 1 shows a Simple Cycle Vapor Compression Refrigeration Plant scheme and the related cycle. Many attempts have been made to reduce the power consumption of the various plants. An amply literature survey on VCRS cycle modifications is given in [3]. Also in [4], a literature review on two-phase ejector applications to VCRS is presented and discussed with COP improvements being analyzed. Cycle modifications for performance improvements have been reported in [5]-[12]. In addition, the adoption of liquid pressure booster has been analyzed and experimented [13]-[15]. Various patents have been applied in this context [16]-[21].

Basic concepts of many tentative consist in the extraction between the condenser and the evaporator – along the expansion process – of liquid in economized vapor injection or vapor in multistage compression refrigeration system [3]. The extracted mass is used to lower the enthalpy at the evaporator inlet and then, it is injected along the compression process. Substantially, the expansion process endpoint can be associated with the liquid Subcooling occurring in the flow exiting from the condenser. The VCRS benefit is connected to the reduced mass flow through the evaporator that has to be compressed. The extracted mass flow needs also to be compressed, however, a power saving is achieved.

The addition of Vapor Pressure Boosters (VPBs) increasing the pressure at the Main Compressor Inlet (MCI) produces a power saving by means of the extracted mass flows, acting as High Pressure Forceful Flows to raise the pressure between the evaporator exit and the MCI. Bleeds and VPBs create the power regeneration of the VCRC.

Fig. 2 shows two liquid bleed Power Regeneration Refrigeration cycle. The two VPBs are two Compressor Expander Groups [22]. An investigation carried out in the Cold Energy Italian Research project context has led to select among the various options the turbomachinery based CEGs as the most suitable [22], [23]. Accordingly, in this paper, the selection of turbomachines leading to the optimum power saving is discussed.

Experimental results obtained by a 100kW Cool Power Cryogenic plant equipped with “ad hoc” selected Bleed Evaporator and CEG turbomachines are presented and analyzed.

G. Cerri is Professor of Fluid Machinery and Energy Conversion Systems, Roma Tre University, Department of Engineering, Via della Vasca Navale, 79, 00146 Rome, Italy (phone: +39 06 57333251; fax: +39 06 5593732/06 57333650; e-mail: cerri@ uniroma3.it).

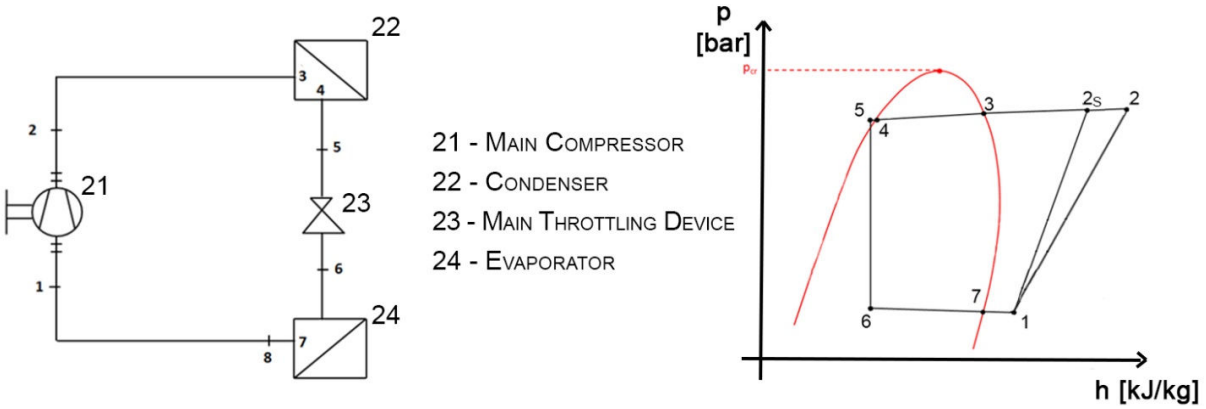


Fig. 1 Simple cycle arrangement

## II. Scientific and Technical Background

To maintain an enclosure at temperatures lower than that of the surrounding, it is necessary to remove the Heat Power entering in. This process can be done using a body surface that has a temperature lower than that of the cold enclosure. Heat Power removal is equivalent to the Cool Power injection. Vapor Compression Refrigeration Plants can accomplish the continuous Cool Power (CP) injection into the Cold Surrounding. Power to compress the Vapor is fed into the compressor. Power and Heat Power (corresponding to the CP) entering are rejected by the condenser into the surrounding.

### *A. Simple Cycle*

VCRPs in Simple Cycle (SC) arrangements are made of four components: evaporator, compressor, condenser and throttling device as shown in Fig. 1 where also the Simple Cycle in the pressure-enthalpy (PH) chart is given.

The SC calculation model is based on the connection among cycle point quantities assuming a succedaneous single component refrigerant (working fluid). Cycle point enthalpies (H) and entropies (S) in the subcooled liquid and superheated vapor (points 1, 2, 5) depend on both pressure and temperature $(p_j, T_j)$. On the saturated liquid and vapor curves (points 3, 4, 7), pressures, enthalpies and entropies are function of the temperatures only ($T_k$). Points inside the liquid-vapor region, temperature ($T_k$) and dryness index ($\delta_{vk}$) are the variables. Thus, the Simple Cycle (SC) can be described as an equivalent one where $T_c = T_3$ and $T_e = T_7$ are the condenser and evaporator temperatures and where the pressure losses are concentrated into the throttling device. Accordingly, $p_2 = p_4 = p_5 = p_3$ and $p_6 = p_7 = p_1$.

Thermodynamic rules allow the calculation of the cooling effect:

$$ce = H(T_e, \Delta T_{sh}) - H(T_5, p_5) \quad (1)$$

The specific compression work being:

$$\Delta H_c = [H(T_c, T_e, \Delta T_{sh}) - H(T_e, \Delta T_{sh})] / \eta_{MC} \quad (2)$$

The heat rejected from the condenser by a working fluid mass unit is:

$$Q_c = ce + \Delta H_c = H(T_c, T_2) - h(T_c, T_5) \quad (3)$$

The working fluid mass flow rate is:

$$m = CP / ce \quad (4)$$

and the overall absorbed power is:

$$P = \frac{CP}{ce} \cdot \Delta H_C \quad (5)$$

The coefficient of performance is:

$$COP = \frac{CP}{P} \quad (6)$$

The model connects the following unknown quantities:

$$X_{SC} = \{p_j, T_j, h_j, s_j, p_k, T_k, h_k, s_k, ce, \Delta H_c, m, P, COP\}$$
$$\text{j} = 1, 2, 2\text{s}, 5 \quad , \quad \text{k} = 3, 4, 6, 7$$

Data are:

$$D_{SC} = \{T_e, T_c, \Delta T_{sh}, \Delta T_{sc}, \eta_{MC}, WF\}$$

$T_e$ is related to the cold enclosure temperature and features and $T_c$ depends on the surrounding temperature.

### *B. Power Regenerated Vapor Compression Cycle*

The Power Regeneration in Refrigeration Plant (PRRP) with two condensate extractions is depicted in Fig. 2, where the cycle is also drawn. Each bleed pressure is reduced to its saturation pressure ( $p_{bi}$ ) then, enters a Bleed Evaporator ( $BE_i$ ) where the liquid evaporates and the vapor is superheated (points 15 and 19). These two processes cause a Subcooling increase of the condensate prior it enters the throttling device

(point 7), downstream of it, the refrigerant passes through the Main Evaporator (from point 8 to point 10).

The cooling effect increases (index 5 in (1) is replaced by 7 (8)), thus, the mass flow rate of the working fluid through the evaporator decreases for constant CP ((4) and (11)).

The refrigerant mass flow rate at the evaporator exit is split in two parts $m_{rc1}$ and $m_{rc2}$ each passing through one Power Recovery Compressor (PRC). Each bleed vapor stream mass flow $m_{bi}$ is expanded through the i$^{th}$ turbine that drives the corresponding Recovery Compressor (RC).

Exit sections of Recovery Compressors and bleed vapor turbines are connected all together to the MCI. Thus, compressor and turbine output pressures are the same and the corresponding streams mix together with the working fluid flow from the evaporator. Due to the Power Recovery Compressors, the MCI pressure becomes higher than that at the evaporator exit.

The PRRP cycle calculations are performed taking equal to 1 kg/s the refrigerant mass flow rate passing through the evaporator and equal to $\mu_{bi}$ the mass fraction of the condensate extracted in the i$^{th}$ bleed. PRRP Enthalpy, Entropy and Pressure for each cycle point can be expressed as for the SC. Additional processes concern the Subcooling contributions, bleed vapor generations, turbine expansions, recovery compressions and mixings of streams entering into the MCI Manifold (MCIM).

The subcooling due to the i$^{th}$ bleed is expressed as:

$$\Delta H_{sci} = \frac{\mu_{bi}(H_{beo} - H_{bei})}{1 + \sum_{e=i}^{b-i} \mu_{bei}} \tag{7}$$

$H_{beo}$ being $H_{15}$ and $H_{19}$, $H_{bei}$ being $H_{13}$ and $H_{17}$. Accordingly, the cooling effect becomes:

$$ce_{RC} = ce_{sc} + \sum_{i=1}^{b} \Delta H_{sci} \tag{8}$$

The shaft equilibrium of each CEG can be expressed as:

$$\mu_{bi} \cdot (H_{tii} - H_{tosi}) \cdot \eta_{Tc} \cdot \eta_{mi} \cdot \eta_{Ci} = \mu_{ci}(H_{cosi} - H_{cii}) \tag{9}$$

$\mu_{ci}$ being the $i^{th}$ fraction of the refrigerant mass flow rate exiting the Main Evaporator.

Mass conservation at the evaporator exit is:

$$\sum_{i=1}^{b} \mu_{ci} = 1 \tag{10}$$

The overall mass flow passing through the Main evaporator is:

$$m_e = \frac{CP}{ce_{RC}} \tag{11}$$

and the mass flow rate entering the MC is:

$$m_{MC} = m_e(1 + \sum_{i=1}^{b} m_{bi}) \tag{12}$$

The enthalpy at the MCI is:

$$H_1 = \frac{\sum_{i=1}^{b} (\mu_{ci} H_{coi} + \mu_{bi} H_{toi})}{1 + \sum_{i=1}^{b} \mu_{bi}} \tag{13}$$

The MC specific work is:

$$\Delta H_{MCRC} = \frac{[H(T_C, p_1, H_1) - H_1]}{\eta_{MC}} \tag{14}$$

and the PRRP absorbed power is:

$$P_{RC} = m_{MC} \cdot \Delta H_{MCRC} \tag{15}$$

and the $COP_{RC}$ being expressed as for the $SC$ substituting in (6) $P_{SC}$ with $P_{RC}$.


Fig. 2 Two Bleed Evaporators (BEs) and two CEGs arrangement

Unknown quantities can be seen as union of two sets, the first one concerns the cycle points and global quantities:

$$X_{CPRC} = \{p_j, T_j, H_j, S_j, p_k, T_k, H_k, S_k, ce_{RC}, \Delta H_{MCRC}, P_{RC}, COP_{RC}\}$$
$$j = 1, 2, 5, 6, 7, 10, 11, 12, 15, 16, 19, 20$$

and

$$k = 3, 4, 8, 9, 13, 14, 17, 18.$$

The second set of unknowns is connected with the power regeneration process:

$$X_{PRC} = \{T_{bi}, \mu_{bi}, \mu_{ci}\},\ i=1, 2, \ldots b$$

Data required to the PRRP model are those listed in the $D_{SC}$ set plus the following:

$$D_{RC} = \{b, T_{bi}, \eta_{ci}, \eta_{ti}, \eta_{mi}, \Delta T_{PPi}, \Delta T_{ai}, T_{beoi}\},\ i=1, 2, \ldots b$$

$\Delta T_{PPi}$ and $\Delta T_{ai}$ being the pinch point and the vapor temperature approach connected with the Bleed Vapor Evaporator heat transfer process whose temperatures versus the exchanged heat is depicted in Fig. 3.

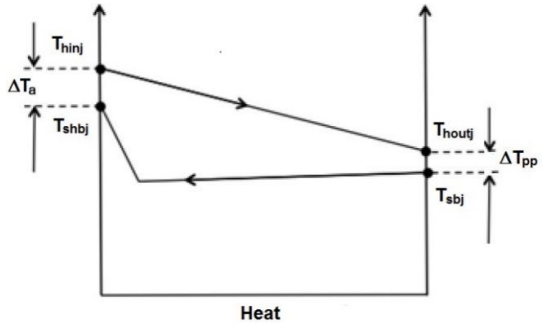


Fig. 3 Bleed evaporator temperature profiles

For any feasible set of $D_{SC} \cup D_{RC}$, the solution can be obtained.

To achieve the best performance (i.e. Minimum of the Main Compressor Power), an optimization procedure can be established using the set:

$$D_{SC} \cup D_{RC} - \xi_{RC}$$

as data and:

$$\xi_{RC} = \{T_{bi}, T_{beoi}\}$$

being degree of freedom to be optimized.

Establishing the values of $\eta_{ci}$ and $\eta_{ti}$ the bleed pressures downstream of the throttling and the superheating degree of each bleed can be optimized according to two concepts:

a- Efficiencies $\eta_{ci}$ and $\eta_{ti}$ can be generically established inside suitable ranges without any turbomachinery selection.

b- Efficiencies $\eta_{ci}$ and $\eta_{ti}$ can be established according to a criterion that takes a technology into consideration and by using similitude concepts to select and modify turbomachine individuals from turbomachinery families characterized by technology.

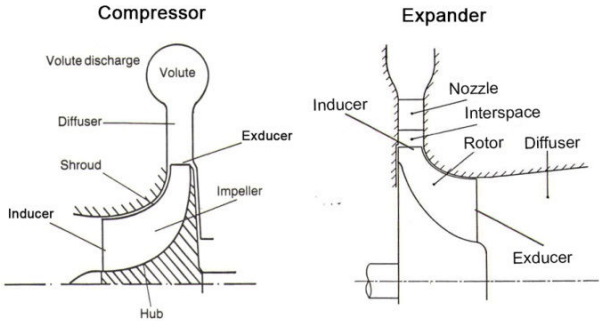


Fig. 4 Compressor and expander through flow section

*C. Turbomachinery Selection*

Models for CEG turbomachine selection, sizing and efficiency evaluation are required for the solution of the optimization process. The outcome is used for the detailed design to build the CEG. The model is based on the concept that for any feasible set of variables (including the efficiencies of turbomachines), the CEG adiabatic expansion and compression processes can be described as function of the thermodynamic quantities of the initial points (turbomachine inlet), local pressure and loss coefficients. For each turbomachinery, the mass flow rates as well as the volumetric flow rates are known. Then, it can be easily understood that the sizing process of the CEGs is based on a trial and error procedure established on compressor and expander efficiencies. Two activity levels concerning a given turbomachinery technology can be identified. The first one concerns with the selection of turbomachinery while the second one consists in the sizing of them for the CEG performance evaluation. Due to the lack of a wide empirical knowledge for this application and the practical absence of a commercially available items, it has been decided the adoption of Car Engine Turbocharger Technology (CETT). They are built in millions of units, they work under severe conditions and they show very good fluid flow performance. Then, high availability, reliability and efficiencies are expected together with low cost for the CEG. Selection has been made taking similitude rules into consideration. Similarity concepts mean that turbomachines, being geometrically similar (i.e. they have the same shape - equal angles), working under kinematic similarity (i.e. triangles of velocity are similar - same vertex angles) and operating with flow fields having the same Reynolds and Mach numbers, show the same efficiencies. According to Fig. 4, geometric through flow section for compressors and turbines, the following variables: $V$ = volumetric flow rate at the inducer for compressor and at the

exducer for expander; $D$ = wheel diameter (exducer for compressor and inducer for expander); $\rho$ = working fluid density; $\mu$ = dynamic fluid viscosity; $C_s$ = working fluid sound speed; $\Delta h_s$ = isentropic enthalpy difference across the machine; $n$ = rotational speed (rpm), have been taken into consideration.

Optimum geometries performance can be described as function of four no dimensional groups: $\omega_s$ = specific angular speed; $D_s$ = specific diameter; $Re$ = Reynolds number and $Ma$ = Mach number. For sufficiently high Reynolds number ($10^6$) losses are almost insensitive to it. Mach number is sufficiently lower than one also shows little influence. In CETT, exhaust expansion takes place at temperatures between 900 and 1200 K and higher while air compression starts around 300 K. R404a sound speed ranges from 140 to 165 m/s. To avoid efficiency penalties, the wheel Mach numbers in turbomachines working with R404a have to be kept lower than the wheel Mach Numbers of high efficiency turbomachines operated with air or exhaust gas. Working fluid R404a sound speed is about 44% of the air when these fluids are compressed. This ratio becomes some 25% when engine exhaust gas and R404a expand. Mach number preservation and similar velocity triangles imply changes in peripheral velocities. Therefore, according to the sound speed ratio in the expander, the rotational speed must change. The ratio between the kinematic viscosity of the air (exhaust) and the one of the R404a ranges from 8 to 40 in this application. Therefore, for equal size turbomachines, the R404a Reynolds number is not relevant. According to the above, only $\omega_s$ and $D_s$ are sufficient to describe performance of geometrically similar machines operating with different working fluids under kinematic similarity (similar triangles of velocity). According to Similitude concepts [24]-[27] of specific speed:

$$\omega_s = \frac{\omega\sqrt{V}}{(\Delta H_s)^{3/4}} \tag{16}$$

and specific diameter:

$$D_s = \frac{D(\Delta H_s)^{1/4}}{\sqrt{V}} \tag{17}$$

have been taken into consideration to establish the empirical relationship:

$$f_{Ds}(\omega_s, D_s, \eta) = 0 \tag{18}$$

that depends on the main flow field shape related to the turbomachine geometry.

In the above equations, $V$ being the inlet volumetric flow for compressors while, $V$ being the exit one for expanders.

A turbomachinery technology (family) is represented by the relationship:

$$f_f(\omega_s, D_s) = 0 \tag{19}$$

that leads to eliminate $D_s$ from (18) and describe the turbomachine (compressor or expander) efficiency as function of $\omega_s$.

Fig. 5 shows the expander efficiency, specific diameter and the product $D_s \cdot \omega_s$ versus specific angular velocity. Points represent measured data and the curve the Best Technology achievements, both for Radial in flow Expander (RE) and for Mixed flow Expander ME.

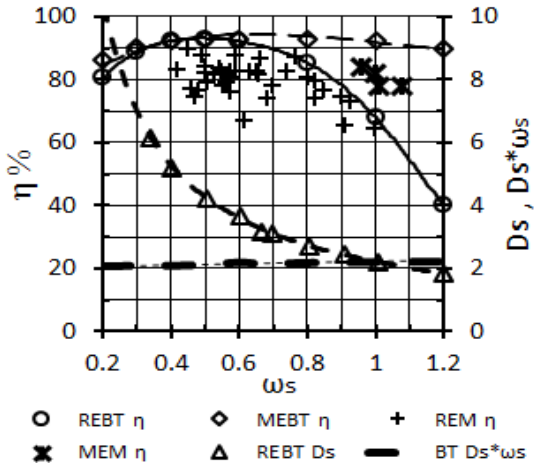


Fig. 5 Expander best technology characteristic versus specific angular speed

For expanders, (19) can be substituted by the product between $\omega_s$ and $D_s$ that leads to express the efficiency as function of the ratio between the peripheral velocity and the spouting one. Such a ratio can be expressed as function of $n$, $D$ and $\Delta H_S$:

$$\frac{U}{C_{SP}} = \frac{\pi \cdot D \cdot n}{60 \cdot \sqrt{2 \cdot \Delta H_S}} \tag{20}$$

This Velocity Ratio (VR) value has to range from 0.60 to 0.80 to reach high efficiencies. At the rotor exit, the adoption of a diffuser adds the rotor exducer pressure as a degree of freedom to adapt the velocity triangles for maximum efficiency. Moreover, for radially oriented rotor blade leading edges, the inlet angle of the relative velocity have to be kept between 45 and 60 degs in respect to the peripheral tangent of the wheel. Always to privilege efficiency partial admission expanders must be avoided, then stator nozzles have to distribute the flow all around the wheel periphery. The radial gap circle of the stator blades trailing edges and the rotor inducer diameter is related to the blade height.

$$\Delta r = k_g \cdot b \tag{21}$$

$k_g$ being a coefficient ranging from 1,.2 to 1.6 depending on the flow Mach number and nozzle geometry. Suggestions contained in [27] are taken into consideration to design a high performance turbine. CETT empirical Data base needs to be

used. Fig. 6 (a) shows a CETT Compressor map and the empirical Data Base. Fig. 6 (b) shows, for a specified pressure ratio, the efficiency, the rotational speed, the specific angular speed and the corrected mass flow rate, versus the volumetric flow rate entering the compressor. Each point corresponds to a wheel of a component of the family associated to an O.E.M. technology. Fig. 6 (c) gives a single CETT wheel performance taken along the maximum efficiency curve that is given by the relationship $\frac{V}{\sqrt{PR-1}} = Const = 0.2838$.

Such data are the efficiency, the pressure ratio, the rotational speed, the specific angular speed, the specific diameter and the Best Technology specific diameter [26] versus volumetric flow rate. In Fig. 6 (d), the same data are reported versus the specific angular speed together with the product between the specific diameter and the specific angular speed. In addition, the Best Technology data are given. Once the compressor wheel type has been selected, it has to be modified according to the following relationships to connect n, *D, V,* and *Δh* that are:

$$k_{ha} \cdot \Delta h_R \cdot n_a^2 \cdot D_a^2 - k_{hr} \Delta h_a \cdot n_R^2 \cdot D_R^2 = 0 \quad (22)$$

for the enthalpy and

$$k_{va} V_R \cdot n_a \cdot D_a^3 - k_{vr} V_a \cdot n_R \cdot D_R^3 = 0 \quad (23)$$

for the volumetric flows. $k_{ha}$, $k_{hr}$, $k_{va}$ and $k_{vr}$, takes differences in angles and slip due to geometry modifications they have to be empirically established [27] to approach the efficiencies of the adopted technology.

Refrigerant working fluid peripheral velocity Mach number

$$M_{aR} = \frac{\pi \cdot n_R \cdot D_R}{60 \cdot C_{SR}} \quad (24)$$

must be less or equal to that of the value for air as working fluid at the rated efficiency point both at the inlet tip diameter ( $D_{itR}$ ) and at the outer wheel diameter.

Many papers and books [24, 25, 26, 27] give the shape ratios and angles for high performance compressor and expander rotors.

One more aspect has to be treated in this section. CETT expander wheels usually are rigidly connected (welded) with the shaft. Since there is a strong reduction in the rotational speed, the expander size is selected taking the torque that the shaft is able to support, thus the following inequality has to be satisfied

$$\frac{\Delta H_{CR} \cdot m_{eR}}{\omega_R} \le Max\left[\frac{m_a \cdot C_{pa} T_a (\beta_a^{\frac{k-1}{k}} - 1)}{\omega_a}\right] \quad (25)$$

the right hand function being the maximum torque that can be calculated using the selected CETT compressor map. It has to point out that the shaft is made of a special alloy (special steel, etc.) and in the CETT high temperature (600°C–900°C) exhaust expands, while in the CEG, the working fluid expands at low temperatures (-70°C to 20°C) representing a further safety factor.

*D. Cycle and CEG Optimization*

Simultaneous optimization of the Power Regenerated Refrigeration Plant to minimize the power consumption for an established Cool Power (CP) has been performed by searching the best variable values for the Power Regeneration process and for the CEG turbomachines. This procedure requires establishing a set of equations:

$$F(D, x, \xi) = 0 \quad (26)$$

and inequalities:

$$I(D, x, \xi) \ge 0 \quad (27)$$

$D$, $x$ and $\xi$ being the data, the unknown variables and the Degree of Freedom (DoF) to be optimized, respectively. $F$ is a vector of equations describing conservation of mass, energy, momentum and entropy, the Working Fluid properties, and auxiliary equations representing the empirical relationships concerning the component performance versus the related variables (i.e. component technology). $F$ includes also equality constraints such as:

$$CP = CP^* \quad (28)$$

$I$ is a vector of inequalities that describe the variable hyperspace domain of definition. $F$ & $I$ establish the calculation models to be solved by a simultaneous solution technique based on cycle and component sizing procedure as described in [28]. Accordingly, the problem becomes:
Search $\bar{\xi}$ that MINIMIZE

$$Fob = MCP \quad (29)$$

Subject to:

$$F(D, x, \xi) = 0 \quad (26')$$

$$I(D, x, \xi) \ge 0 \quad (27')$$

The solution scheme is shown in Fig. 7. It is organized as big blocks, each made of various modules according to [28].

This solution method requires establishing a suitable Objective Function ( $Fob$ ) minimization process being constrained by the equation set (26) and by conditions expressed as inequalities (27). The optimized solution leads to establish also the $\mathbf{g_{ci}}$ and $\mathbf{g_{ei}}$ sets of geometric variables of the components influencing the objective function. Parallel design processes led to establish the other component sizes.

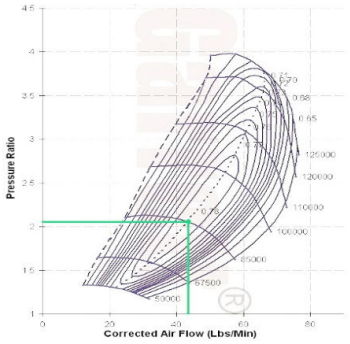


Fig. 6 (a) Compressor map

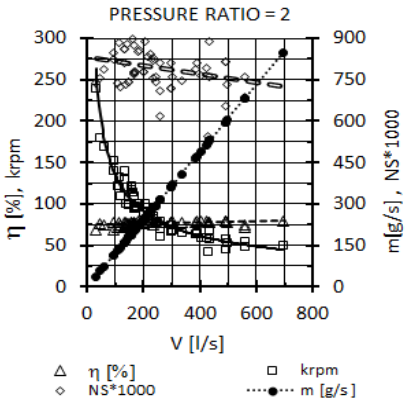


Fig. 6 (b) CETT database

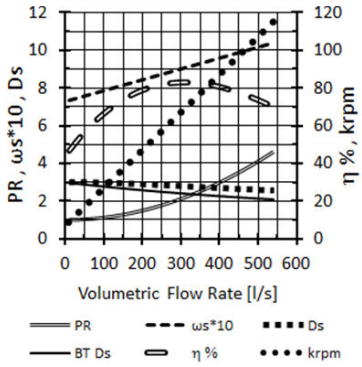


Fig. 6 (c) Compressor performance versus volumetric flow rate

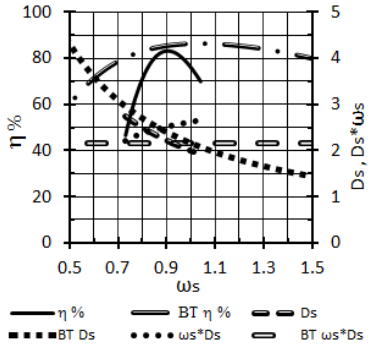


Fig. 6 (d) Efficiency & specific diameter versus specific speed

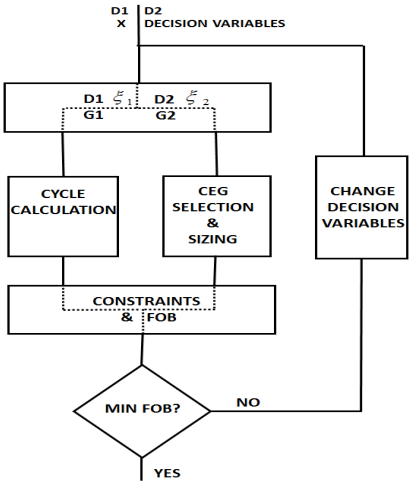


Fig. 7 Block scheme of the overall solution and optimization method

Innovative aspect of this research activity is the selection of the Compressor and Expander units to arrange the Compressor Expander Groups (CEGs) by choosing and modifying items included in an available turbomachinery technology. The process is schematically represented in Fig. 7. The MCP represents the $Fob$ to be minimized given the **D** set.

Concerning the Degree of Freedom (DoF) the following can be stated:

- $\Delta T_{ppj}$ and $\Delta T_{Aj,}$ being the pinch point and the approach temperature differences in the BVGs, lower they are lower the MCP is. Reducing such temperature differences, the sizes of the BVGs become larger and larger increasing also the initial costs of the plant. The right compromise consists in establishing the lower bounds for them ($\Delta T^{l}_{ppj}$ and $\Delta T^{l}_{Aj}$);
- b, being the number of bleeds; the higher b, the lower MCP. Increasing b, the MCP step reduction becomes lower and lower while the plant initial cost rises. Thus, b (1 to 3) can be assumed depending on the application;
- ΔTsbj  j=1-b, being the saturation temperatures of the bleed inside each jth BVGj can be optimized to achieve the best $Fob$;
- $\omega_{csj,}$ being the specific angular speed of each j compressor to be selected, leads to the geometry selection of turbomachinery to achieve the best efficiency of the j$^{th}$ CEG ( $\eta_g = \eta_{cj} \cdot \eta_{ej} \cdot \eta_{mj}$). Thus, $\omega_{csj}$ optimum values have to be searched.

Including the turbomachinery modifications of the selected compressor and expander models, it is possible to establish the geometric unknown quantities embedded in the set $\boldsymbol{g_c}$ and $\boldsymbol{g_e}$ for compressor and expander respectively.

Moreover, also $rpm$, $\eta_{cj}$, $\eta_{ej}$ and $\eta_{mj}$ are evaluated. Thus,

$$X_{CEG} = \{g_{ci}, g_{ei}, rpmi, \eta_{ci}, \eta_{ei}, \eta_{mi}\},\ i = 1, 2, \ldots b$$

degree of freedom for the BT or for the CETT are

$$\xi_{CEG} = \{\omega_{csi}\}$$

taking into consideration that a CEG is made by a compressor and an expander rigidly connected by a shaft.

## III. Cryogenic Plant Optimization

A 100kW Cool Power Cryogenic Plant operating between $T_e$ = -40°C, $T_c$ = +40°C, $\Delta T_{sh}$ = 5°C, $\Delta T_{sc}$ = 5°C using R404a as refrigerant working fluid arranged with a power regeneration section made of two bleeds equipped with one CEG as shown in Fig. 8.

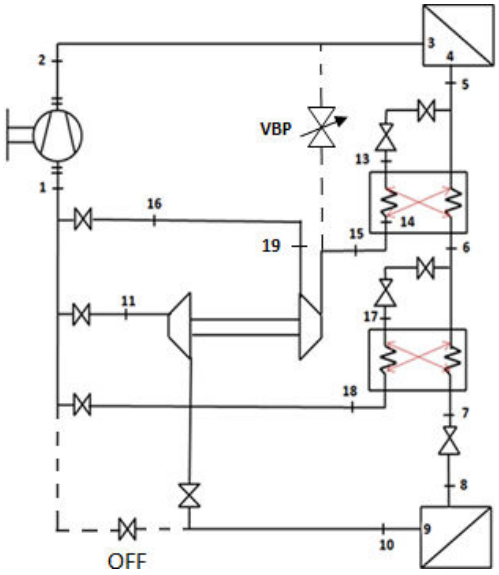


Fig. 8 Scheme of the demonstrator layout

Calculations have been performed for four cases: Simple Cycle (as reference); one bleed (1B1CEG); two bleeds with two CEGs (2B2CEG); two bleeds with one CEG (2B1CEG), the second bleed being discharged after the heat transfer device directly into the Main Compressor inlet manifold. Result comparisons are shown in Table I where in the columns cases that have been elaborated are given and in the rows there are the plant quantities. It can be observed that in all the IPRC cases the MCP has strong reduction in respect to the SC. The adoption of two bleeds with one CEG installed on the highest Pressure bleed and the second bleed being used for condensate Subcooling purposes and being injected downstream of the HPB Recovery Compressor, in the MC inlet section, has been chosen as demonstrator plant.

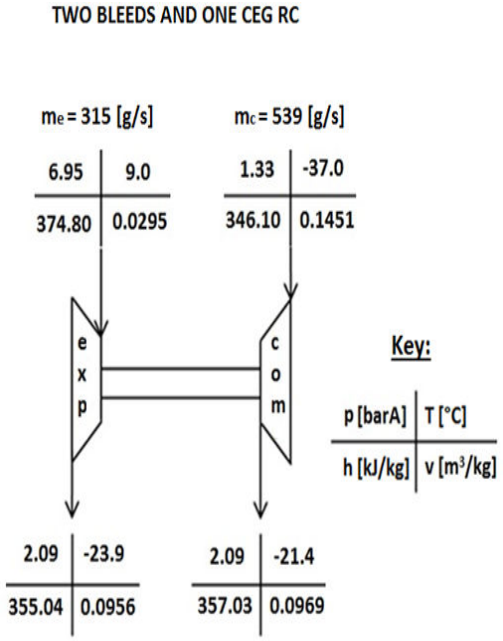


Fig. 9 CEG optimized thermodynamic and flow data

The optimized 2B1CEG scheme is shown in Fig. 8 and has been calculated by the above methodology. The CEG data are given in Fig. 9. A vapor by-pass connects the MC exit to the Expander to have the possibility of modifying the CEG rotational speed establishing a fast starting procedure. According to the simulated results, a test bench based on the scheme of Fig. 8 has been designed; components have been manufactured and assembled together to set up the test bench. The various sections are briefly illustrated in the following.

TABLE I
Optimum Calculations of IPRC Options

| A | B | C | D | E | F | G | H |
|---|---|---|---|---|---|---|---|
| QUANTITY | SC | 1B1CEG | (C-B)/B % | 2B1CEG | (E-B)/B % | 2B2CEG | (G-B)/B % |
| QC [kW] | 100.00 | 100.00 | 0 | 100.00 | 0 | 100.00 | 0 |
| Pmc [kW] | 101.50 | 78.53 | -23 | 74.98 | -26 | 74.31 | -27 |
| COP [-] | 0.98 | 1.27 | 30 | 1.33 | 36 | 1.35 | 38 |
| Δhce [kJ/kg] | 84.18 | 142.71 | 70 | 178.20 | 112 | 168.21 | 100 |
| mmc [kg/s] | 119 | 1.06 | -11 | 1.05 | -12 | 1.07 | -10 |
| mb1 [kg/s] | - | 0.36 | - | 0.31 | - | 0.32 | - |
| mrc1 [kg/s] | - | 0.70 | - | 0.56 | - | 0.54 | - |
| mb2 [kg/s] | - | - | - | 0.18 | - | 0.15 | - |
| mrc2 [kg/s] | - | - | - | - | - | 0.06 | - |

*A. Compressor Wheel Selection*

Since the inducer blade angle being unchanged and the refrigerant incidence angle as to be equal to that of the air best efficiency, the selection is made according to the specific speed (i.e. similar inlet velocity triangles and inlet flow shapes). Among the various candidates, the choice has been made taking into consideration the exducer diameter. It has been machined to accommodate both the total enthalpy rise and the exit volumetric flow to have similar triangles of velocity. Photos of Fig. 10 show the compressor wheel after modification; the left hand rotor blades have been cut. In addition, the casing rear and front disks with the inlet duct are given in the same figure.

*B. Expander Wheel and Shaft Assembly*

Expander wheel is rigidly welded with the shaft. It has to be selected taking the torque to be transmitted into account, because the shaft running speed is rather low in respect to the original spinning owing to Mach number preservation. Thus, the shaft stem has been selected accordingly.

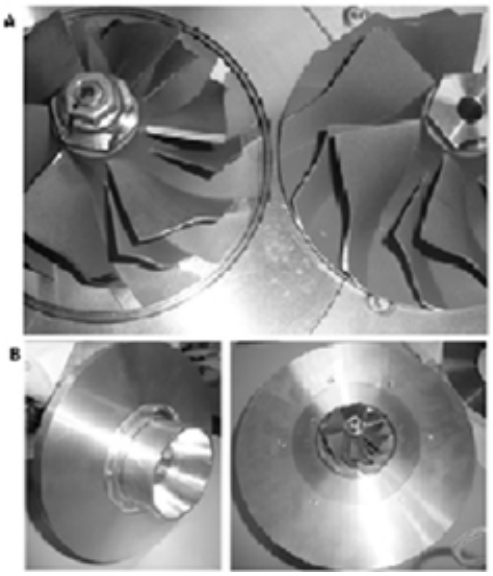

Fig. 10 Photos of compressor wheel (a), front & rear disks (b)

Refrigerant operational temperatures are strongly reduced in respect to a traditional turbocharger one. This is in favor of stability and safety. Sizes of the turbine inducer and exducer have been modified to meet the efficiency goal. Since the selected Expander Wheel and Shaft assembly establish the exit angle, it has been possible to calculate the exit pressure and triangles of velocity at any exducer diameter, taking into consideration the diffuser that is required to lower the axial velocity to about 10 m/s introducing a further degree of freedom.

Since the flow angles at the rotor exit are known for any selected wheel, given the volumetric flow at the exducer exit, the tip diameter can be calculated. Inducer blade height is established by the flow angle at the rotor inlet and by the related volumetric flow. Nozzle vanes have been designed to reach the required velocity and the flow angle at the rotor inlet. Losses depend on the nozzle exit angle, on the channel length and passage size and shape.

Nozzle blade trailing edge circle is suitably located upstream of the rotor leading edge circle. Fig. 11 shows two set of nozzle blades tested on the bench: the right side blades have been designed and tested under supersonic exit conditions, while the left side ones under subsonic and transonic exit flows. Moreover, a diffuser is located downstream of the exducer station to allow the best selection of the expander wheel exducer pressure that contributes to the wheel exit velocity triangle shape and size. A ball bearing housing has been adopted mainly for two reasons: The first is related to the low losses produced by the angular ball bearing cartridge and the easy repair; the second is related to the lubrication aspects. The test bench is equipped with an oil lubrication system. The oil is the same used for main compressors of cryogenic plants. Theory and Tests made in the Roma Tre lab have shown that such an oil can safely be used to lubricate the bearings. Moreover, lubrication analyses have shown that also liquid R404a can behave as safe lubricant in this application.

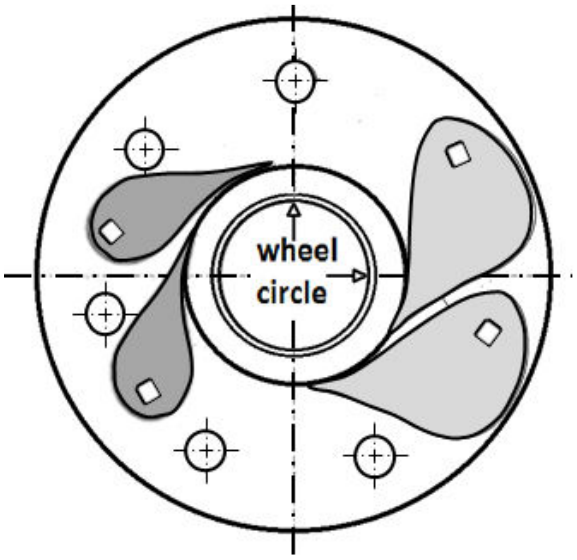


Fig. 11 Turbine nozzle vane arrangements

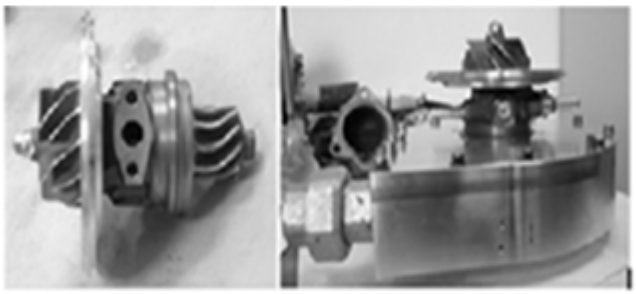

Fig. 12 Details of the Compressor Expander Group

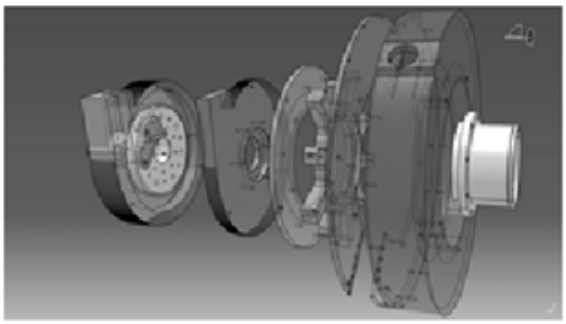

Fig. 13 CEG exploded 3D representation

Fig. 12 shows details of the CEG assembly and the expander inlet duct. Fig. 13 shows an exploded 3D drawing of the CEG components.

The CEG has been tested on a Roma Tre compressed air operated test bench (see Fig. 14). It has demonstrated the capability of continuous and safe running. Moreover, the air test results have been used to predict the CEG performance when the working fluid would be a succedaneous one of the R404a. Such a forecast performance has demonstrated that the built CEG would be capable to satisfy the needs for the R404a 100kW Cool Power Test bench.

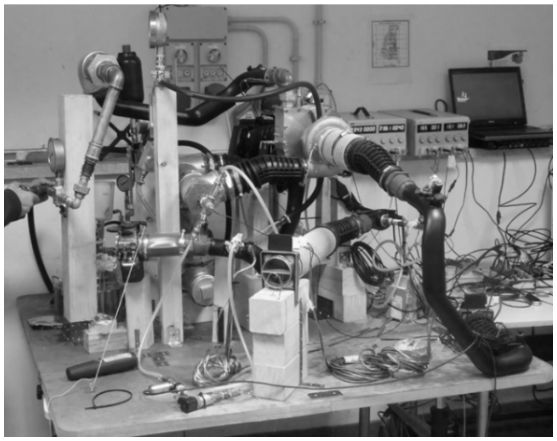

Fig. 14 Compressed air operated test bench

*C. Performance Tests and Results*

The test bench for 100kW cool power has been equipped with the CEG. A photo of the whole bench is shown in Fig. 15. The test bench has been operated under Simple Cycle arrangement to evaluate the reference conditions.

At this research stage, the Test bench MC availability was for about 50kW cool power. Therefore, steady state conditions allowed the CEG to run under the derated behavior at some 20 krpm. Thus, a sudden step opening of the condenser by-pass valve carried on full load CEG running tests.

Fig. 16 shows the pressure differences across the expander and the compressor versus the rotational speed. It can be seen that at the rotating velocity from 30 krpm to 40 krpm the pressure increase produced by the Recovery Compressor ranges from 50kPa to 100kPa. The expander pressure drop ranges from 4 to 5 bar when the rotational speed ranges from 33 to 40 krpm. Both these results are in the design expected values. Tests made keeping the condenser by - pass valve off, and operating the bleed valves to maintain the calculated superheating the test bench behaves under steady state conditions. The CEG velocity has been led at some 20 krpm producing a 20kPa pressure increase. The pressure drop across the expander has been some 150kPa. The test cool power was some 52 kW. Steady State speed versus expander mass flow is given in Fig. 17, circle point represents the Steady State run at 20000 rpm with about 700 kg/h (194,4 g/s). Triangle point represents the predicted point corresponding to the circle one, when the CEG machines would behave under similarity conditions at the nominal loading. Such values correspond to 100kW test bench cool power.

Main Compressor Power saving, in respect to that consumed in simple cycle arrangement is shown in Fig. 18. During the steady state behavior of the test bench that makes the CEG run under derated conditions, the circle point can evidence some power saving of 10% – 12%. In addition, in this case, the behavior, for 100kW cool power has been simulated under similarity conditions.

Fig. 15 The test bench

Some 18%-22% MCP saving has been predicted. The triangle point spot reports such a forecast. As soon as possible tests to validate the 100kW cool power test bench behavior will be performed when the adequate MC will be available. The plant cycle has been optimized to achieve the minimum MCP consumption by using the above-described models, procedures and methodologies. Quantities that have been assumed for the design are: working Fluid R404a; $T_c$=40°C; $T_e$= -40°C; $\Delta T_{sh}$=5°C; $\Delta T_{sc}$=5°C; $\Delta T_{ppj}$=30°C; $\Delta T_{Aj}$=30°C; b=2; The Main Compressor efficiency has also been assumed according to the applications in the field. The well-established Simultaneous Solution Methodology used by Roma Tre Fluid Machinery and Energy Conversion Systems Group (FM & ECSG) [28] has been used to accomplish evaluations.

Moreover, during the test, the lubrication has been changed from oil to the liquid R404a. No problems arose for more than ten hours until the system was stopped for inspection and evaluation.

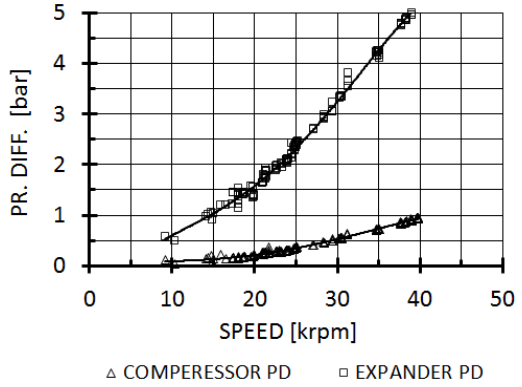


Fig. 16 Pressure difference versus rotational speed

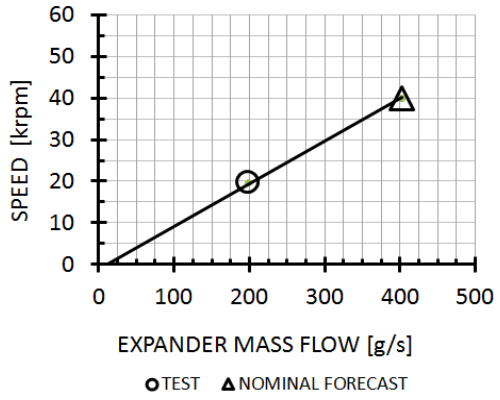


3

Fig. 17 Speed versus expander mass flow

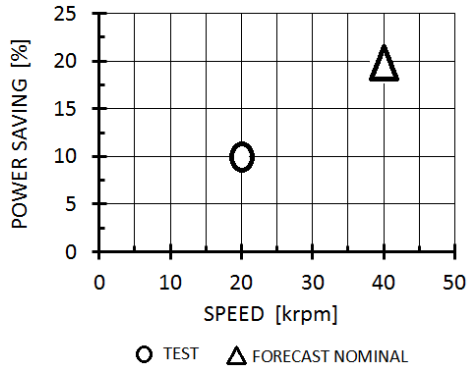


Fig. 18 Main compressor power saving versus rotational speed

## IV. Conclusion

The selection and the sizing methodology adopted to design Compressor Expander Group Turbomachines to be components of Power Regenerated Refrigeration Plant has been demonstrated to be a valid tool to get the optimized solutions.

Tests on a cryogenic plant equipped with one CEG designed for optimum performance have been carried out. The Car Engine Turbocharger Technology selected and re-sized compressor has demonstrated its correct behavior increasing the R404a pressure versus rotating speed in agreement with the prediction.

The CETT selected and re-sized expander has shown to be able to work under derated conditions as expected. Predicted full load behavior taking the test results under derated conditions (50% load) into account shows a very good energy saving. Moreover, liquid R404a can be used as lubricant for the ball bearing cartridge without having drawbacks.

## Acknowledgements

The Authors acknowledge the Italian Ministry for the Environment, Land and Sea; Angelantoni Industries S.p.A.; Se.Te.L S.r.l. and Roma Tre University for the COLD ENERGY Project Support.

## Nomenclature

*Symbols*

| | |
|---|---|
| B | Bleed |
| B | Pressure Ratio |
| Cs | Sound Speed |
| $C_{SP}$ | Spouting Velocity |
| Δ | Difference |
| D | Data, Diameter |
| ξ | Degree of Freedom |
| Ds | Specific Diameter |
| ⍰ | Efficiency |
| $g_c$ | Geometric Variables of the Components |
| $g_m$ | Geometric Shape |
| H, h | Enthalpy |
| m | Mass Flow Rate |
| M | Measured |
| Ma | Mach Number |
| μ | Dynamic Viscosity; Mass Fraction |
| n | Rotational Speed (rpm) |
| ν | Kinematic Viscosity |
| $\omega_s$ | Specific Speed |
| $\omega_{sc}$ | Specific Speed of Compressor |
| P | Power |
| p | Pressure |
| Re | Reynolds Number |
| ρ | Density |
| δ | Dryness Index |
| S, s | Entropy |
| T | Temperature |
| U | Peripheral Velocity |
| V | Volumetric Flow |
| WF | Working Fluid |
| X | Unknown Quantities |
| $Z_b$ | Number of Bleeds |

*Subscripts*

| | |
|---|---|
| a | approach, air |
| b | bleed, blade, blade high |
| c | compressor, condenser |
| ce | cooling effect |
| E, e | expander, evaporator, exit |

| | |
|---|---|
| h | enthalpy |
| i, j, k | order number |
| i | inlet |
| m | mechanical |
| mc, MC | main compressor |
| o | Out |
| pp | pinch point |
| R | Refrigerant |
| rc | recovery compressor |
| RC | Recuperated Cycle |
| s | Specific, isentropic |
| sc | simple cycle |
| sh | superheating |
| t | Turbine, tip |
| v | Vapor, Volumetric Flow |

*Acronyms*

| | |
|---|---|
| BT | Best Technology |
| BVGs | Bleed Vapor Generators |
| CE | Cool Environment |
| ce | Cooling Effect |
| CEG | Compressor Expander Group |
| CETT | Car Engine Turbocharger Technology |
| CFD | Computational Fluid Dynamic |
| COP | Coefficient of Performance |
| CP | Cool Power |
| DoF | Degree of Freedom |
| FM & ECSG Group | Fluid Machinery and Energy Conversion Systems |
| HP | Heat Power, High Pressure |
| IP | Intermediate Pressure |
| LP | Low Pressure |
| MC | Main Compressor |
| ME | Main Evaporator, Main Flow Expander |
| MCI | Main Compressor Inlet |
| MCP | Main Compressor Power |
| OF | Objective Function |
| PR | Pressure Ratio |
| PRC | Power Recovery Compressor |
| PRRP | Power Regeneration Refrigeration Plant |
| PRS | Power Recovery System |
| RC | Recovery Compressor |
| RE | Radial Expander |
| SC | Simple Cycle |
| VCRC | Vapor Compression Refrigeration Cycles |
| VCRS | Vapor Compression Refrigeration Systems |
| VPB | Vapor Pressure Booster |
| VR | Velocity Ratio |

## REFERENCES

[1] Borlein, Energy Savings in Commercial Refrigeration Equipment: Low Pressure Control, *White paper, Schneider Electric*; August 2011.

[2] New Refrigeration Cycle to Improve 100 – Year - Old Technology. *Calmac Manufacturing Corporation*; October - December 2001.

[3] N.Q. Minh, N.J. Hewitt and P.C. Eames, Improved Vapor Compression Refrigeration Cycles: Literature Review and Their Application to Heat Pumps. *International Refrigeration and Air Conditioning Conference*. Paper 795; 2006.

[4] J. Sarkar, Ejector Enhanced Vapor Compression Refrigeration and Heat Pump Systems - A Review, *Renewable and Sustainable Energy Reviews* 16, 6647-6659; August 2012.

[5] J. Yu, H. Zhao and Y. Li, Application of an Ejector in Auto Cascade Refrigeration Cycle for the Performance Improvement, *International Journal of Refrigeration,* vol.31, pp.279-286; 2008.

[6] Y. Zhu and P. Jiang, Hybrid Vapor Compression Refrigeration System with an Integrated Ejector Cooling Cycle, *International Journal of Refrigeration*, vol.35, pp. 68-78; 2012.

[7] A. Selvaraju and A. Mani, Experimental Investigation on R134a Vapor Ejector Refrigeration System, *International Journal of Refrigeration*, vol.29, pp.1160-1166; 2006.

[8] L. Kairouani, M. Elakhdar, E. Nehdi and N. Bouaziz, Use of Ejectors in a Multi-Evaporator Refrigeration System for Performance Enhancement, *International Journal of Refrigeration,* Vol.32, pp.1173-1185; 2009.

[9] A. Prakash, Improving the Performance of Vapor Compression Refrigeration System by Using Sub–Cooling and Diffuser, *International Journal of Engineering, Business and Enterprise Applications*, ISSN (Print): 2279-0020, IJEBEA 13-129; 2013.

[10] K.H. Reddy et al., Improvement of Energy Efficiency Ratio of Refrigerant Compressor, *International Journal of Scientific & Technology Research*, Volume 2, ISSN 2277-8616, Issue 5; May 2013.

[11] E. Elgendy, Parametric Study of a Vapor Compression Refrigeration Cycle Using a Two-Phase Constant Area Ejector, *International Journal of Mechanical, Aerospace, Industrial and Mechatronics Engineering,* Vol.: 7 No: 8; 2013.

[12] N. Upadhyay, To Study the Effect of Sub-Cooling and Diffuser on the Coefficient of Performance of Vapour Compression Refrigeration System, *International Journal of Research in Aeronautical and Mechanical Engineering,* Vol. 2, Issue. 6, pgs. 40-44; June 2014.

[13] D.T. Reindl and H. Hong, Evaluation of Liquid Pressure Amplifier Technology, *International Journal of Air Conditioning and Refrigeration*, vol.13, pp.119-127; 2005.

[14] A. Hadawey, Y.T. Ge and S. A. Tassou, Energy Saving Trough Liquid Pressure Amplification in a Dairy Plant Refrigeration System. *CEBER Brunel University Uxbridge Middlesex*, UB8 3PH, UK.

[15] DOE, Liquid Refrigerant Pumping Technology for Improving Refrigeration Performance and Capacity, *New Technology Demonstration Program*, U.S. Department of Energy

[16] M.F. Taras, A. Lifson and T.J. Dobmeier, Refrigerant Cycle with Tandem Economized and Conventional Compressors. *United States Patent*; Patent No.: Us 6.955.058 B2; Date of Patent: Oct.18, 2005.

[17] M.J. Andres, Expendable Turbine Driven Compression Cycle Cooling System, *United States; Patent Application Publication*; Pub. No.: Us 2007/0193301 A1; Pub. Date: Aug.23, 2007.

[18] A. Lifson and M.F. Taras, Refrigerant System with Variable Capacity Expander. *United States; Patent Application Publication*; Pub. No.: Us 2010/0031677 A1; Pub. Date: Feb.11, 2010.

[19] J.W. Bush, W.P. Beagle and B. Mitra, Refrigerating System with Parallel Staged Economizer Circuits Using Multistage Compression, *United States; Patent Application Publication;* Pub. No.: Us 2010/0223938 A1; Pub. Date: Sep.9, 2010.

[20] B. Mitra, W.P. Beagle and J.W. Bush, Refrigerating System with Parallel Staged Economizer Circuits Discharging to Interstage Pressures of a Main Compressor, *United States; Patent Application Publication*; Pub. No.: Us 2010/0223939 A1; Pub. Date: Sep.9, 2010.

[21] M. Ascani, Refrigerating Device and Method for Circulating a Refrigerating Fluid Associated With it, *United States Patent*; Patent No.: Us 8,505,317 B2; Date of Patent: Aug.13, 2013.

[22] M. Ascani, G. Cerri and E. De Francesco, Power Reduction in Vapour Compression Cooling Cycles by Power Regeneration, *The 69th Conference of the Italian Thermal Machines Engineering Association*, ATI2014, September 10 – 12, 2014.

[23] G. Cerri, Sviluppo di un impianto per produzione del freddo criogenico mediante rigenerazione e sviluppo del gruppo scambiatore-espansore-compressore *ational* (SEC), *Compressors and Expanders State of the Art Technical Report OR2 – A2.2 SEC Cold Energy Project*, 2012.

[24] S.L. Dixon, CA. Hall, Fluid Mechanics and Thermodynamics of Turbomachinery, *Butterworth Heinemann*, Sixth Edition, 2010.

[25] O.E. Baljè, Turbomachines: A Guide to Design, Selection, and Theory, *John Wiley and Sons*, New York; 1980.

[26] A. Whitfield, N.C. Baines, Design of Radial Turbomachines, *John Wiley and Sons*, New York, USA; 1990.

[27] G. Cerri, Organic Fluid Turbines for Various Engine Power Level Turbochargers, *The 33rd ASME International Gas Turbine and Aeroengine Congress*, ASME pap. 88–GT–1, Amsterdam, Netherlands, June 5 – 9, 1988.

[28] G. Cerri, A Simultaneous Solution Method Based on a Modular Approach for Power Plant Analyses and Optimized Designs and Operations, *International Gas Turbine and Aeroengine Congress,* ASME paper 96–GT–302, Birmingham, UK, June 10–13, 1996.